The Semi-Analytic Mode Matching Algorithm for GPR Wave Scattering from Multiple Complex Objects Buried in a Dielectric Soil Half Space

Ann W. Morgenthaler and *Carey M. Rappaport*
Northeastern University, Boston, MA 02115
rappaport@neu.edu

***Abstract* —** The Semi-Analytic Mode Matching (SAMM) algorithm is a quick and efficient computational method that can model wave scattering from multiple objects in half spaces. This algorithm relies heavily on the appropriate choice of coordinate scattering centers (CSCs) for its modal expansions. Here, the radius of curvature method of finding CSCs is extended to "tune" the CSC loci. Because the CSC locations are essentially frequency independent and do not depend strongly on the dielectric contrast between scatterer and background, it is worthwhile to carefully analyze particular scattering object shapes and store the optimal CSC locations for future use. Scattering from multiple targets buried within half spaces can be constructed from simpler simulations of the individual targets taken independently in uniform media – combining these initial simulations correctly can greatly reduce overall computational time and increase robustness in the full simulations. Excellent results are obtained by comparing SAMM and Finite Difference Frequency Domain (FDFD) for multiple buried 2D scattering objects 0.1 – 15 wavelengths in size.

.

INTRODUCTION

The Semi-Analytic Mode Matching (SAMM) algorithm [1] is used to model single frequency scattering from complex-shaped 2D dielectric objects buried within half-space geometries by numerically matching all boundary conditions at discrete "fitting points" spanning the objects' perimeters and portions of the half space boundary. Singular value decomposition (SVD) is used to minimize the residual of the linear function $\mathbf{F} \cdot \mathbf{c} - \mathbf{b}$, where $\mathbf{c}$ is a vector of unknown mode coefficients, $\mathbf{b}$ is vector which describes the mismatch in each boundary condition at every fitting point along all interfaces in the modeled region, and $\mathbf{F}$ is the dense, nonsquare matrix which relates them.

The key to the SAMM algorithm is choosing the locations of the multiple coordinate systems about which sets of modes are expanded, and a method using the radii of curvature (ROC) associated with the scatterer fitting points is described in [2] for single targets in uniform backgrounds. In this paper, we describe how to extend this procedure to multiple objects and demonstrate how a complex scattering problem may be broken into smaller, simpler pieces, each of which can be combined to form an initial guess for the full scattering problem. The SAMM algorithm converges more rapidly and accurately using an intelligent starting solution than if the full problem is simulated in one pass.

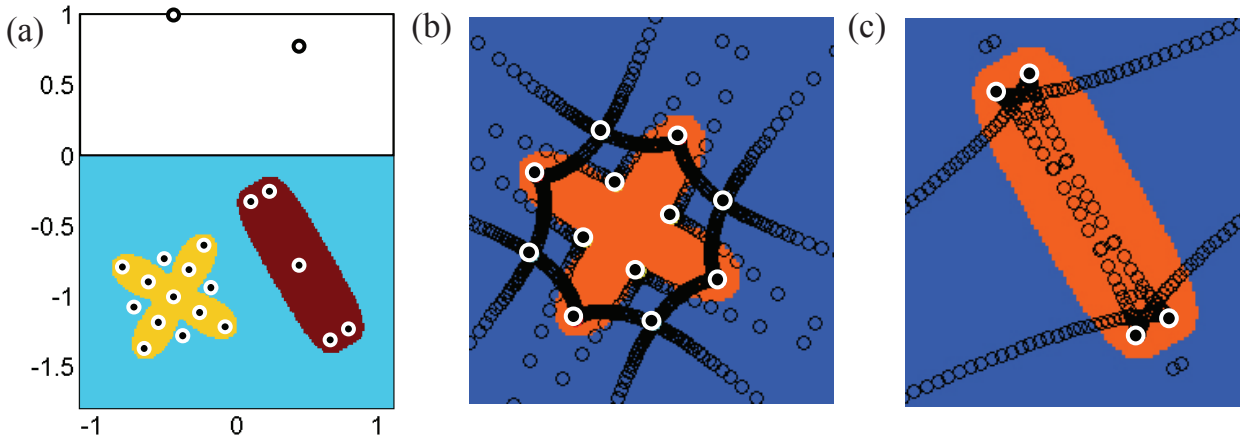

Figure 1: (a) Test geometry showing optimal target CSCs (white rimmed black circles) and image CSCs (black rimmed white circles). The "plus sign" and hyperellipse scatterers have complex dielectric values $\varepsilon = 20\varepsilon_0$ (1+ i 0.051) and $\varepsilon = 10\varepsilon_0$ (1+ i 0.051), respectively, and are buried in dry sand with $\varepsilon = 2.55\varepsilon_0$ (1+ i 0.001). (b) Close up of ROC points (black circles) for the plus sign scatterer and the CSCs (white rimmed circles) selected from these points. Four interior ROC-CSCs are located in the arms of the plus sign. Four exterior ROC-CSCs are found at the junctions of the arms but these are too close to the target. The intersections of the ROC branches are possible candidates for exterior CSCs but the in fact the optimal locations of the exterior CSCs will be along the line segments connecting the exterior ROC-CSCs and the ROC branch intersections. (c) Close up of the ROC points for the hyperellipse scatterer (black circles) and the interior ROC-CSCs (white rimmed circles) selected from these points. No exterior CSCs are needed for this convex shape.

IMPROVING THE CSC LOCATIONS

Whereas convex targets require only interior CSCs, concave targets will need both interior and exterior CSCs to achieve accurate results with the SAMM algorithm. Interior ROC-CSCs are those ROC points (X_q, Y_q) which both lie within the scatterer and have corresponding lengths ℓ_q from (X_q, Y_q) to the object centroid which are local maxima such that $\ell_q > \ell_{q\pm1}$. Exterior ROC-CSCs are those ROC points which both lie outside the object and have lengths which are local minima: $\ell_q < \ell_{q\pm1}$.

Additionally, the locations outside the scattering object where the ROC curves cross may be suitable for exterior CSC status. However, we find that ROCs which lie either too close or too far away from the scatterer boundary are not particularly good choices for CSCs; in the former case, the Hankel function singularity generates such large fields within the target that substantial errors arise from the singular value matrix decomposition of **F**. In addition, for objects with large aspect ratios, more CSCs are required; a rough rule of thumb is that an *R*: 1 rectangle requires *R* CSCs to maintain the same error level as a single CSC in a 1:1 square. A test scattering geometry is shown in Fig. 1(a), and the complex "plus sign" scatterer is shown in Fig. 1(b) with details of its ROC curves. The plus sign is an example of a shape where a naïve choice of CSCs will not result in optimal scattering, though the hyperellipse scatterer in Fig. 1(c) is well modeled by its 4 interior ROC-CSCs plus a CSC at the hyperellipse center.

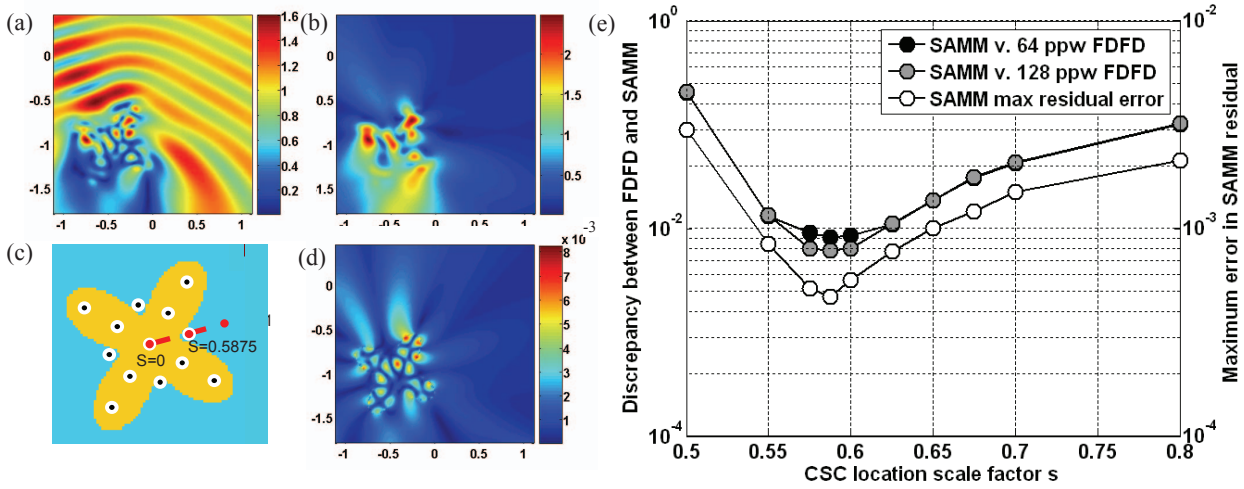

Figure 2: (a) SAMM simulation of the total electric field E_z for a 300 MHz TM plane wave source normally incident from above on a plus sign shaped scatterer placed in a uniform dry sand background using the CSCs in (c) with s = 0.5875. (b) SAMM simulation of the scattered electric field, found by subtracting the incident, reflected, and transmitted plane waves from the total field in (a). (c) Locations of CSCs for the plus sign scatterer, scaled by s, where s = 0 at the center of the object, s = 0.4505 at the exterior ROC-CSC locations and s = 1 where the ROC curves cross, as in Fig. 1(b). (d) Difference between SAMM and 64 point per wavelength FDFD calculations of the magnitude of E_z. (e) Plots of the difference between the SAMM and FDFD simulations and a plot of the maximum residual error in the SAMM algorithm, all as a function of the exterior CSC scaling parameter s, showing how well the curves track each other; s = 0.5875 is the optimal choice using either metric.

To optimize the exterior CSC locations for the plus sign in a uniform dielectric, we simulate scattering with the SAMM algorithm using a scalable parameter s, shown in Fig. 2(c), where s = 0.4505 is the exterior ROC-CSC location and s = 1 is the location where the ROC curves cross. The value s = 0.5875 turns out to be the optimum location for the exterior CSCs, determined both by comparing the SAMM simulations to very finely gridded reference Finite Difference Frequency Domain (FDFD) solutions of either 64 or 128 points per wavelength and also by computing the absolute value of the biggest component of the residual vector $\mathbf{F} \cdot \mathbf{c} - \mathbf{b}$ in the SAMM simulations. Both methods of analyzing the error in the SAMM algorithm are plotted in Fig. 2(e) as a function of s, with the implication that CSC locations may be optimized directly using the SAMM algorithm without needing to compare SAMM results to those generated by another numerical method. A SAMM simulation of the total and scattered electric field for the optimal choice of exterior CSCs is plotted in Fig. 2(a) and (b). The difference between SAMM and the 64 point per wavelength FDFD solution is plotted in Fig. 2(c), where the maximum difference between the two is less than 1%. A similarly good result is found for SAMM simulations of the hyperellipse in uniform background material.

BUILDING MULTI-TARGET SOLUTIONS FROM SINGLE OBJECT SOLUTIONS

Combining the optimal SAMM scattering solutions for individual targets in uniform backgrounds to create an initial guess to the more complicated two-object buried object problem, we simulate this latter

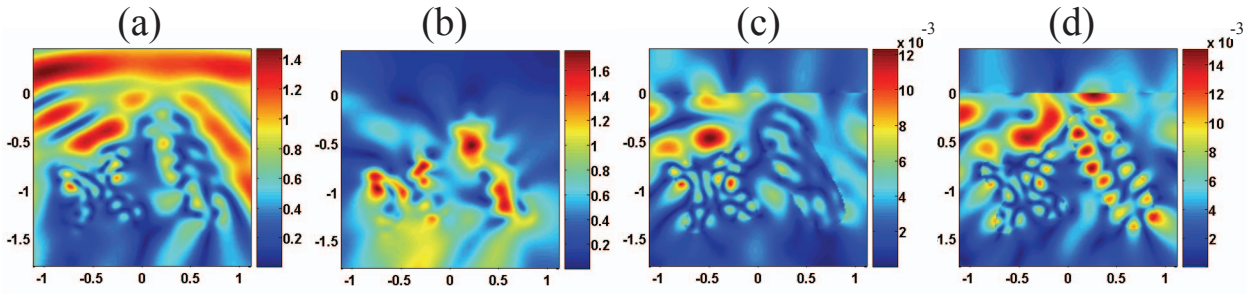

Figure 3: (a) Total E_z field from a 300 MHz plane wave source normally incident from air on a dry sand half space in which the two targets of Fig. 1(a) are buried, calculated by combining the fields from each target computed separately in infinite dry sand to make an initial guess. (b) Scattered E_z field, computed by subtracting the incident, reflected and transmitted plane waves from the total field in (a). (c) Difference between the SAMM calculation in (a) and a 64 point per wavelength FDFD simulation of the same geometry. (d) Difference between the direct SAMM simulation where no initial guess is used and the 64 point per wavelength FDFD simulation.

problem by adding image CSCs above the half space boundary as shown in Fig. 1(a). A single image CSC per scatterer, located the same distance above the boundary as the centroid of the scattering object is located below it, results in scattering fields which are almost as accurate as those in the object-in-infinite-background simulations. Although it is also possible to use SAMM to simulate the entire problem in one step (typically more modes are required for convergence and a less accurate solutions is the final result), we expect that with greater complexity and larger numbers of scatterers, it will be increasingly important to construct an initial guess for the SAMM algorithm by combining the electromagnetic fields from simpler sub-problems. Fig. 3 is comparison of the plus sign-hyperellipse half space simulation with and without initially-constructed approximate fields. If used, these starting fields are created from simple linear combinations of the sub-problem scattered fields and the incident, reflected, and transmitted plane waves. In both cases, maximum differences between SAMM and reference FDFD solutions of 1-2% are found. With these new enhancements to the SAMM algorithm, combined with its existing ability to quickly model subsurface scattering in all types of realistic media, SAMM is a very attractive general-purpose forward modeling tool ideally suited for half space inverse scattering applications [3].

REFERENCES

[1] Morgenthaler, A. W. and C. Rappaport, "Scattering from Lossy Dielectric Objects Buried Beneath Randomly Rough Ground: Validating the Semi-Analytic Mode Matching Algorithm with 2D FDFD," *IEEE Trans. Geosci Rem Sens* **39**:11, Nov. 2001, pp. 2421-2428.

[2] Morgenthaler, A. W. and C. Rappaport, "GPR Wave Scattering from Complex Objects using the Semi-Analytic Mode Matching Algorithm: Coordinate Scattering Center Selection", in review for *IEEE Trans. Geosci Rem Sens* Special 2010 *IGARSS* issue.

[3] Firoozabadi, R., E. Miller, C. Rappaport, and A. Morgenthaler, "A New Inverse Method for Subsurface Sensing of Object Under Randomly Rough Ground Using Scattered Electromagnetic Field Data," *IEEE T Geosci Rem Sens* **45**:1, Jan 2007, pp. 104-117.